Spring 5-17-2019

Microfluidic Assessment of Stem Cell-Derived Pancreatic Beta Cells

Arvind Rajamani Srivatsava
Washington University in St. Louis

Washington University in St. Louis

McKelvey School of Engineering

Department of Biomedical Engineering

Microfluidic Assessment of Stem Cell - Derived Pancreatic β Cells

By

Arvind Rajamani Srivatsava

A thesis presented to the McKelvey School of Engineering of Washington University in St. Louis in partial fulfillment of the requirements for the degree of Master of Science

May 2019

St. Louis, Missouri

Acknowledgement

I would like to sincerely thank my advisor, Dr. Jeffrey Millman and my lab members at the Millman lab for their continued help, patience, support and encouragement throughout my project.

I would also like to thank my parents and my uncle for their support and advice which empowered me to pursue my thesis in the Millman Lab.

Arvind Rajamani Srivatsava

Washington University in St. Louis

May 2019

Table of Contents

List of Tables

List of Figures

Abstract of the Thesis

Microfluidic Assessment of Stem Cell-Derived Pancreatic β Cells

by

Arvind Rajamani Srivatsava

Master of Science in Biomedical Engineering Washington University in St. Louis, 2019

Research Advisor: Professor Jeffrey Millman

Contemporary and traditional methods of perifusional analysis of cells, pancreatic β cells in particular, involve the utilization of costly equipment exhibiting difficulties in setup and inflexibilities in operation and application. Microfluidic devices in general are inexpensive, easy to fabricate and are capable of screening multiple microenvironmental conditions, with the potential to generate concentration gradients for the study of biological phenomena such as cell migration. Utilization of these devices for cellular fluorescence imaging is also possible, paving the way for more sophisticated methods of dynamic assessment. Herein, we fabricated a pre-designed microfluidic device from photolithography, containing microwells capable of immobilizing human β islet or stem cell-derived β cells for perifusional analysis with low (2mM) and high (20mM) concentrations of glucose, following subsequent dynamic estimation of insulin produced using the insulin ELISA. The main aim was to compare and contrast insulin secretory behavior of human islet and stem cell-derived β cells with dynamic study of calcium ion activity during insulin exocytosis through fluorescence imaging, using an alternative method of assessment, namely, microfluidics.

Chapter 1

Introduction and Background

1.1. Diabetes Mellitus and B Cell Function

Diabetes Mellitus (DM) is one of the most rapidly growing diseases and is a group of metabolic disorders which leads to the inability of the body to regulate blood glucose levels (Mohammed et al. 2009). It comprises of Type-1 DM, which is autoimmune and involves the degeneration and destruction of insulin-secreting pancreatic β cells located in the islets the Langerhans leading to an insulin deficiency (Mohammed at al. 2009, Pagliuca et al. 2014) and Type - 2 Diabetes. The latter leads to insulin resistance in peripheral tissues such as the muscle and adipose, which further leads to reduction in insulin secretion caused by glucotoxicity and lipotoxicity as a result, later during the course of the disease (Mohammed at al. 2009). Type -1 diabetes (T1D) is currently one of the most prominent diseases in the United States and the rest of the world, with about 1.25 million Americans currently living with T1D comprising 200,000 youth less than 20 years of age and more than 1 million adults who are 20 years and older (*JDRF*). Around 40,000 people a year in the United States are diagnosed with T1D, and an estimated 5 million people are expected to be diagnosed with the disease by the year 2050 (*JDRF*). Considering these odds, research around the treatment of this disease is of vital importance and highly necessary at this point of time. Intensive insulin therapy was treated as an effective method to reduce complications arising from T1D. One of the elements of this involved a multi-component program with administration of “continuous subcutaneous

insulin infusion (CSII)" (Hirsch et al. 1990) injections coinciding with each meal on a 24-hour day (Kirsch et al. 1990). However, since this could not emulate the normal pulsatile insulin secretory pattern in the native human β cell and it comes with the risk of hypoglycemia, it is not considered the most effective method of treatment (Mohammed et al. 2009). Other treatments, such as donor pancreatic transplantation were also looked at as viable options for the treatment of the disease and reduce hypoglycemic episodes, the procedure was ultimately limited by its high morbidity and mortality rates (Mohammed et al. 2009).

Another method of treatment currently employed is the transplantation of cadaveric human islets. Patients who were transplanted with these islets could remain insulin independent for 5 years or longer (Pagliuca et al. 2014). Since the scarcity and quality of such islets were the major limitations to this method, it may not have been considered a mainstream viable method of treatment. On the other hand, an unlimited supply of stem cell derived β cells could be differentiated from stem cells and could serve as treatments for millions of patients through transplantation procedures to a vascularized location in the body coupled with immunoprotection (Pagliuca et al. 2014). Stem cell derived β cells, owing to their uniform and consistent supply, could also serve as specimens for diabetes drug design and discovery, unlike cadaveric human islets, which were scarce, exhibited high variability from donor to donor due to various reasons such as cause of death, genetics, etc (Pagliuca et al. 2014).

Concerning the current experimental analysis, two different types of pancreatic β cells were used: Human-derived β cells which were sourced from cadaveric pancreas, and stem cell derived β cells, synthesized and produced in the Millman Lab. This experiment focuses on the calcium ion signaling

and insulin secreting properties of both of these kinds of cells, in response to glucose stimulation. The function of insulin is to keep the blood glucose levels within the natural limits by regulating glucose uptake by muscle and fat cells as well regulating the hepatic glucose output (Leibiger et al. 2008) or gluconeogenesis from lactate and amino acids. Insulin release comprises of the packaging of insulin in secretory granules (small and ~0.3um in diameter), the movement of these granules towards the plasma membrane, the exocytotic fusion of the granules with the plasma membrane and the subsequent retrieval of the secreted membranes by endocytosis (Rorsman et al. 2003). Both human islets and the stem cell derived (SCD) β cells have different mechanisms that trigger insulin secretion, both of which release insulin in different quantities equivalent to the concentration of glucose in the blood, and in this case, the perfusing fluid, and this mechanism is often referred to as the stimulus-secretion coupling (Leibiger et al. 2008).

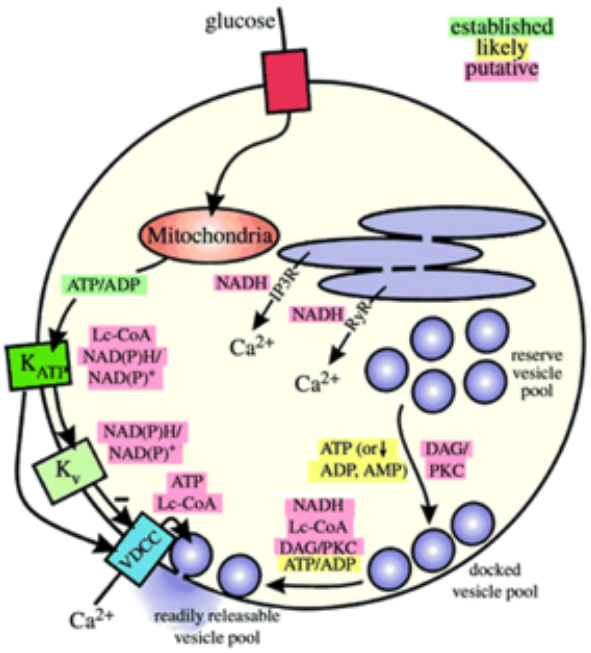

Figure 1.1. Human Islet Insulin Release Mechanism. Mechanism of insulin release from islet β cells upon stimulation with glucose. (Sourced from Macdonald et al. 2005)

In human islet (HI) β cells, the insulin secretion mechanism upon glucose stimulation first begins with the facilitated diffusion of high extracellular glucose through the glucose transporter protein, GLUT-2 into the cell. The subsequent ATP molecules produced through glycolysis of glucose and subsequent metabolism causes an increase in the ATP/ADP ratio, which triggers the closing of K^+ channels. This leads to the accumulation of intracellular potassium ions which results in an overall positive potential difference between the inside of the cell and outside, which in turn triggers the opening of voltage-gated Ca^{2+} ion channels leading to the influx of calcium ions into the cell. This influx of calcium ions into the cell induces the exocytosis of the insulin granules [Figure. 1.1.]. The SCD β cells, which are hiPSC-derived, work similarly to adult Human islets in sensing changing glucose concentration, with subsequent membrane depolarization and calcium influx and

accumulative behavior with the release of insulin granules through the function of glucose transporter proteins, metabolic enzymes and potassium ion channels (Pagliuca et al. 2014). Insulin secretion response is typically characterized to have two phases [Figure. 1.2.], the first phase being a large spike occurring 1-3 minutes after glucose stimulation (Mohammed et al. 2009), attributed to the exocytosis of readily releasable insulin granules close to the plasma membrane which release insulin in response to nutrient and non-nutrient secretagogues (Wang et al. 2009), followed by the second phase of insulin release, where the insulin quantity reduces to a suprabasal level and continues to increase gradually as long as external glucose stimulation persists (Mohammed et al. 2009). The second phase of secretion is explained by the intracellular granules or vesicles mobilizing and beginning to dock and fuse with the t-SNARE sites on the plasma membrane (Wang et al. 2009), from where insulin exits the cells.

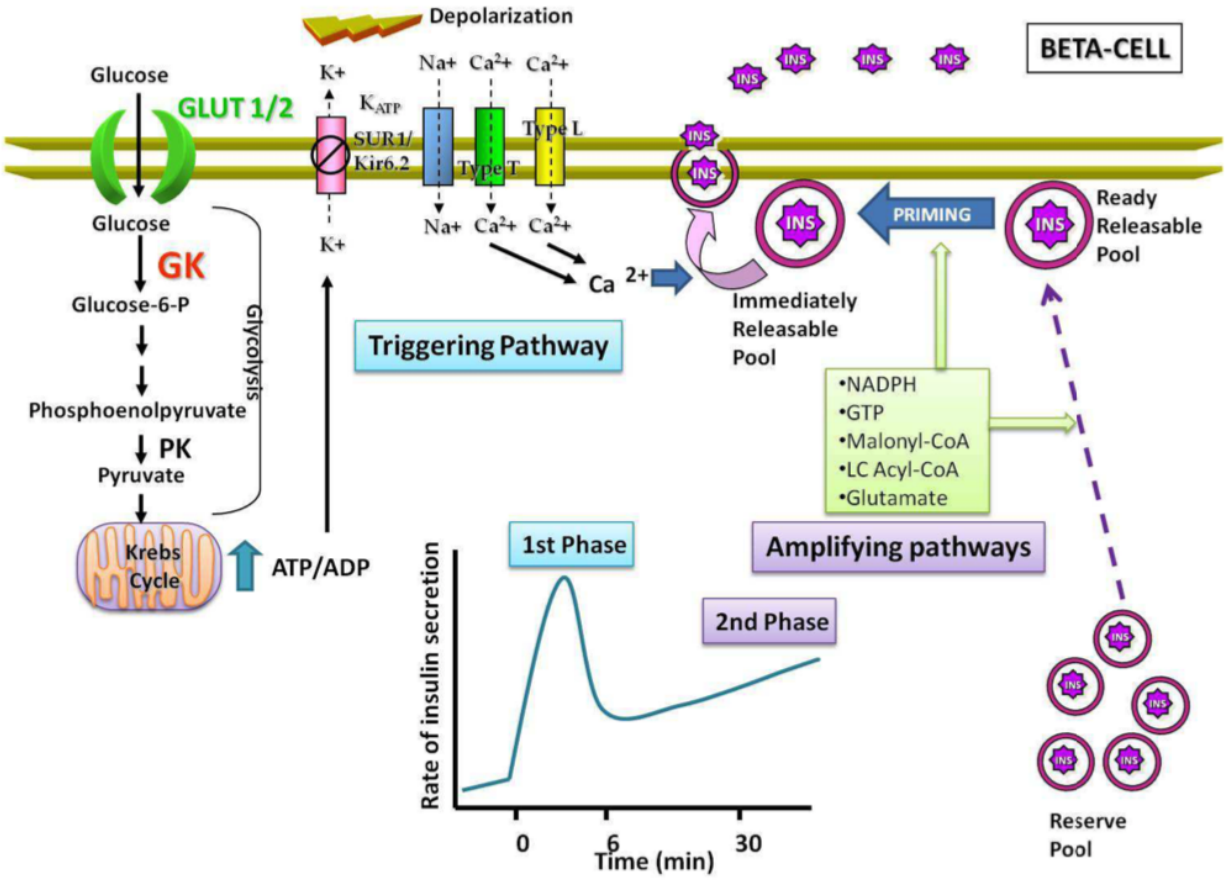

Figure 1.2. Biphasic Response of Insulin. Illustration of the biphasic insulin secretion response, sourced from Popa et al. 2013

Insulin secreted in response to glucose stimulus is traditionally measured using the Insulin Enzyme-Linked Immunosorbent Assay (ELISA). This involves the binding of insulin to a primary antibody, the complex formed in turn is bound with a secondary antibody, after disposing of the solution containing excess primary antibody. The samples are then treated with a TMB substrate (3,3,5,5 - tetramethylbenzidene) which is a visualizing reagent that binds with secondary antibody complexes and stains the solution in various intensities of the color blue depending indirectly on the

concentration of insulin in the sample. Not only is this process time consuming, the reagents and ELISA plates required to run this procedure are also expensive. This assay may not yield a large range of dynamic resolution since it is impractical to calculate the instantaneous concentration of insulin (it would require too many samples, whose analysis would also be time consuming and very expensive) rather than that of samples collected over small intervals of time. Since the insulin release activity in both of these kinds of cells are similarly linked to the calcium ion influx activity, it becomes almost imperative to target studies towards analyzing the calcium release profile as a way of indirectly measuring the viability of SCD β cells and Human islets alike. This form of dynamic assessment of ion and cellular activity only aids to get a deeper understanding of the functional gap between both these kinds of pancreatic β cells.

1.2. Microfluidics and Perifusional Analysis

Microfluidics can be defined both as the science of study of fluids through micro-channels, or as the technology of manufacturing micro-miniaturized devices containing various chambers and convolutions through which fluids are confined (*Elveflow*). A microfluidic chip consists of a pattern of microchannels which are designed and brought about through molding or engraving, the most prominent method of fabrication being through the use of photolithography. This pattern or network is in turn linked to several holes of different dimensions punched or drilled through the chip, which serve as inlets or outlets through which it is connected to the macroenvironment by the help of tubes and other fluid transporting equipment (*Elveflow*). This way, fluids are directed through the device in order to achieve efficient levels of mixing, automation and high throughput systems. The micropatterns achieved in microfluidic devices can be precisely designed in a way beneficial to the type of purpose, providing the ability to assess a myriad of experimental conditions in tandem with

one another, offering substantial parameter control, thereby being a more efficient method of analysis (*Elveflow*). Another advantage of microfluidic devices is the relatively smaller volumes of fluids, reagents and other chemicals involved, thereby reducing the cost of operation drastically. These also have the potential to process and analyze samples with very minor sample handling, allowing the user to generate multi-step reactions requiring a lot of functionalities, but a low level of expertise. These advantages, coupled with their uncomplicated, ever-improving and swift methods of fabrication, make them a prevailing contemporary tool of choice for several different areas of research interest, such lab-on-chip devices, which handle picolitres of fluids and comprise of a more complex architectures, cell biology studies and in protein crystallization - a faster analysis involving staging several different viable microenvironmental conditions, as well as in other areas such as micro fuel cells, drug screening and chemical microreactors, etc.

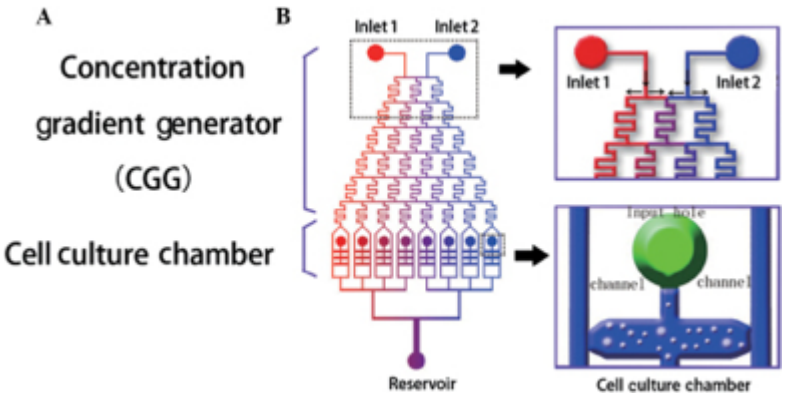

Figure 1.3. Microfluidic Concentration Gradient Generation. A microfluidic design capable of generating user-dictated concentration gradients. (Sourced from Yin et al. 2015)

In the case of this perifusional analysis, a typical dynamic perifusional system would comprise of a peristaltic pump pushing a perfusing fluid through a sample container containing the cells under

study, the perfusate being collected from this chamber in a 96 well plate, which is programmed to move automatically according to the number of sample containers in use and the preset sampling rate [Figure. 1.4.i)-ii)]. Microfluidic devices find their advantages where traditional systems meet their limitations: the latter of which being expense, difficulty in setting up and operation - a plethora of technical requirements necessary in order to run the systems themselves (Mohammed et al. 2009). Moreover, traditional perifusional systems can often be linked with mechanical perturbation of the cells under study, inducing stress and hence limiting the maximum functional capability of the specimens (Mohammed et al. 2009). In addition, microfluidic devices are capable of generating user-described chemical concentration gradients (Adewola et al. 2010) [Figure. 1.3.], as well as setting up multiple microenvironmental conditions in different channels of the device, which are monumental for cell migration studies (for example, chemokine chemotaxis) and other biological studies as well. The presence of parallel microchannels enable the running of multiple experiments and a composition of clear and transparent materials like PDMS make microfluidic devices capable of dynamic optical fluorescence imaging, which set themselves apart from all the previous methods of perifusional analysis.

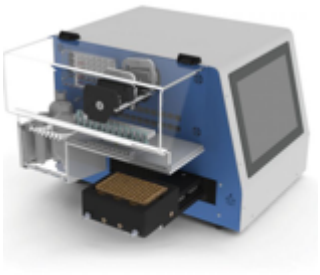

Figure 1.4. Perifusion Equipment. Image of a traditional perifusion system (Sourced from *Biorep*)

Static analysis of islet function can be achieved through islet multiplexing in a 96 well plate, although this being a static method, it only warrants the measurement of bulk insulin produced by the cells (secretory capacity) and does not provide insight on the temporal dynamics of insulin secretion, comprising of the biphasic response of insulin secretion over time (Mohammed et al. 2009). In order to study the dynamics of insulin secretion, we chose to employ, fabricate and recreate a pre-designed microfluidic device to quantify the dynamic insulin secretion profile of both human pancreatic β cells and stem cell-derived β cells, as well as for subsequent calcium fluorescence imaging. The device comprises of three layers [Figure. 1.5.] - one containing several microwells (diameter 500 um and depth 150 um) designed to immobilize the cells and reduce the amount of surface area exposed to flow (Mohammed et al. 2009), the second containing a large reservoir which serves to efficiently mix the fluids entering the device through the inlets drilled in the simple third layer. The design of the reservoir and the microchannels in the second layer ensures minimum shear force imparted to the cell specimens as well as exposes them to a slowly moving body of fluid of changing chemical concentrations. This simple design specifically allows for the efficient perifusional analysis of the pancreatic β cells and provides scope for multiple experiments

to be conducted after simple cleaning procedures with milliQ water and 70% ethanol (Adewola et al. 2010).

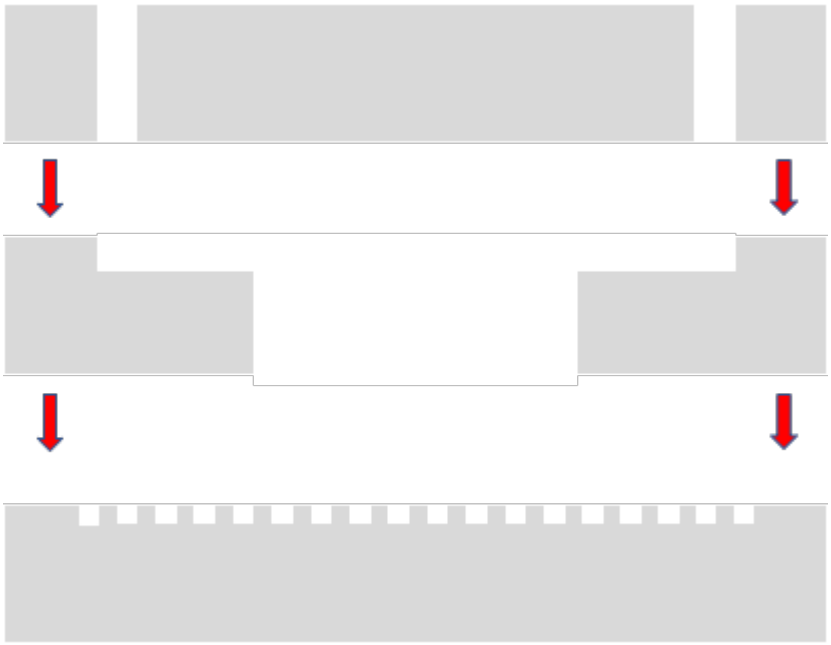

Figure 1.5. Device Layer Diagram. Illustration of the layers of the designed PDMS Microfluidic device (bottom to top): first layer containing the microwells to immobilize islets, second layer containing fluid reservoir and third layer containing inlets and outlets.

1.3. Fluorescent Staining and Calcium Fluorescence Imaging

Fluorescence imaging is one of the most efficient methods of analyzing and advancing the knowledge of cellular biology at the molecular level. In vivo fluorescence imaging is a non-invasive method that produces images in “real-time” and is capable of fast data acquisition times. It involves the excitation of a fluorophore within the specimen, by a photon of low wavelength, and its subsequent emission of a light of higher wavelength (The difference in excitation and emission wavelengths referred to as the Stokes shift), due to the return of the outermost electrons in a fluorophore molecule to their ground state after reaching a higher elevated orbital state on absorbing the incident photon. The emitted photon is then captured by a detector camera for further analysis (Hassan et al. 2004) [Figure. 1.6.].

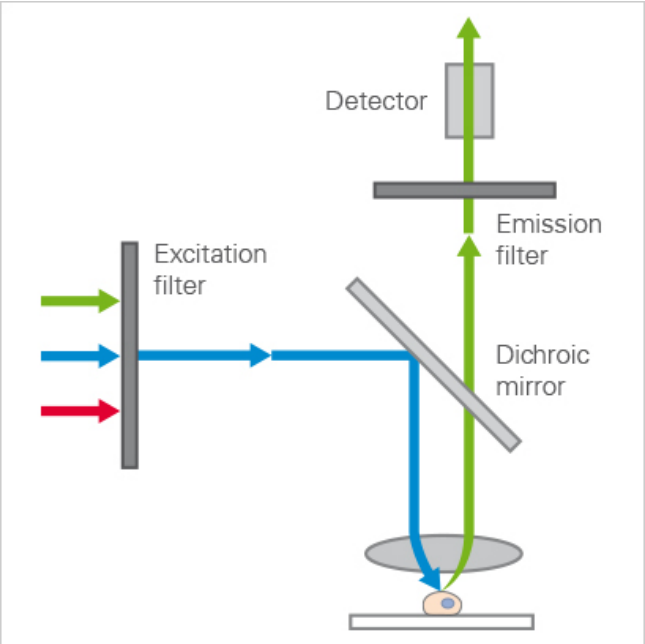

Figure 1.6. Fluorescence Microscope. Simple illustration of light pathways in a fluorescence microscope, sourced from *Ibidi*

Fluorescence imaging finds its use among a myriad of biological applications. More specifically, Ca^{2+} is targeted very often for research studies, owing to it being a "ubiquitous intracellular messenger that regulates multiple cellular functions such as secretion, contraction, cellular excitability and gene expression in all organ systems" (Russell et al. 2011), and hence targeting and analyzing calcium ion activity could be considered a key to understanding several cellular and other biological processes in the body. Calcium fluorescence imaging, in general, involves the usage of fluorophores which specifically bind with calcium ions to form fluorescent complexes whose responses compound into a fluorescence emitted signal captured by a microscope or macroscope camera. It serves as a efficient tool for in situ imaging of cellular activity and function in different organ systems, the brain being one of the prominent areas of application (Russell et al. 2011).

More relevant to our application, since the insulin stimulus-secretion coupling in HI and SCD β cells is directly linked to the mobility of calcium ions, it becomes possible to analyze this flux behavior by means of imparting fluorescence and capturing these changes in fluorescence at different stages of stimulation. This was achieved through the use of calcium ion-binding green fluorescent dye, Fluo-4 AM, which can be incorporated into the cells through a low glucose KRB (Krebs-Ringer Buffer) staining process. In the insulin secretion pathway, Fluo-4 AM binds with calcium ions which enter the cells before the insulin granules are released, forming Fluo-4 - Ca^{2+} complexes which have altered optical properties and appear green spots of light (emission wavelength ~ 540 nm) when excited with blue light of wavelength ~488 nm (Gee et al. 2000). The relative green fluorescence intensity is dependent on the concentration of calcium ions entering the cells, which in turn depends on the strength or concentration of the stimuli, which are in this case, glucose and KCl for control.

Figure 1.7. Imaging Equipment. Zeiss Axio Zoom V16 fluorescence microscope used in our fluorescence imaging experiment, sourced from *Zeiss*.

Other dyes such as Fura-2 have also been used for calcium fluorescence imaging, and Fura-2 being a ratiometric dye, helps in the direct estimation of calcium ion concentration by first obtaining a calibrated calcium ion signal. Fluo-4 AM on the other hand, is usually employed for observing and measuring relative changes in the fluorescence intensity signal and hence relative changes in calcium ion concentration, which is sufficient for the purposes of our study. Fluo-4 finds use in many applications such as flow cytometry, confocal laser scanning microscopy and microplate screening assays (Gee et al. 2000). With regard to the current study, it serves as an excellent assessment tool owing to its high rates of cell permeation and the ability to quantify cellular Ca^{2+} changes over a very broad range of concentration (Gee et al. 2000).

Chapter 2

Photolithography and Device Preparation

2.1. Introduction and Results

One of the most common methods to design and fabricate a microfluidic device involves the use of Photolithography [Figure 2.1]. It is a process that uses high intensity light and a photomask to prepare a network of polymer on a silicon wafer (Berkowski et al. 2009). This polymer network is formed through a physical change to the photoresist, containing a photosensitive compound and a mixture of polymers that become soluble or insoluble after exposure to UV light (Berkowski et al. 2009). Two types of photoresists exist: positive and negative. A positive photoresist comprises of an insoluble polymer that turns soluble in the presence of UV light, while the negative kind of photoresist is composed of a soluble polymer turning insoluble, due to polymerization and crosslinking, in the presence of UV. The photoresist used in this experiment is SU-8 2050 which is a negative photoresist. The reason for using this is accredited to its stable mechanical, thermal and chemical characteristics, and it can be coated in thicknesses greater than 1mm (Lee et al. 2015). It is also used in a variety of other applications owing to its capability of being patterned into to make tall microstructures with high aspect ratios, which is unprecedented in conventional photoresists (Lee et al. 2015).

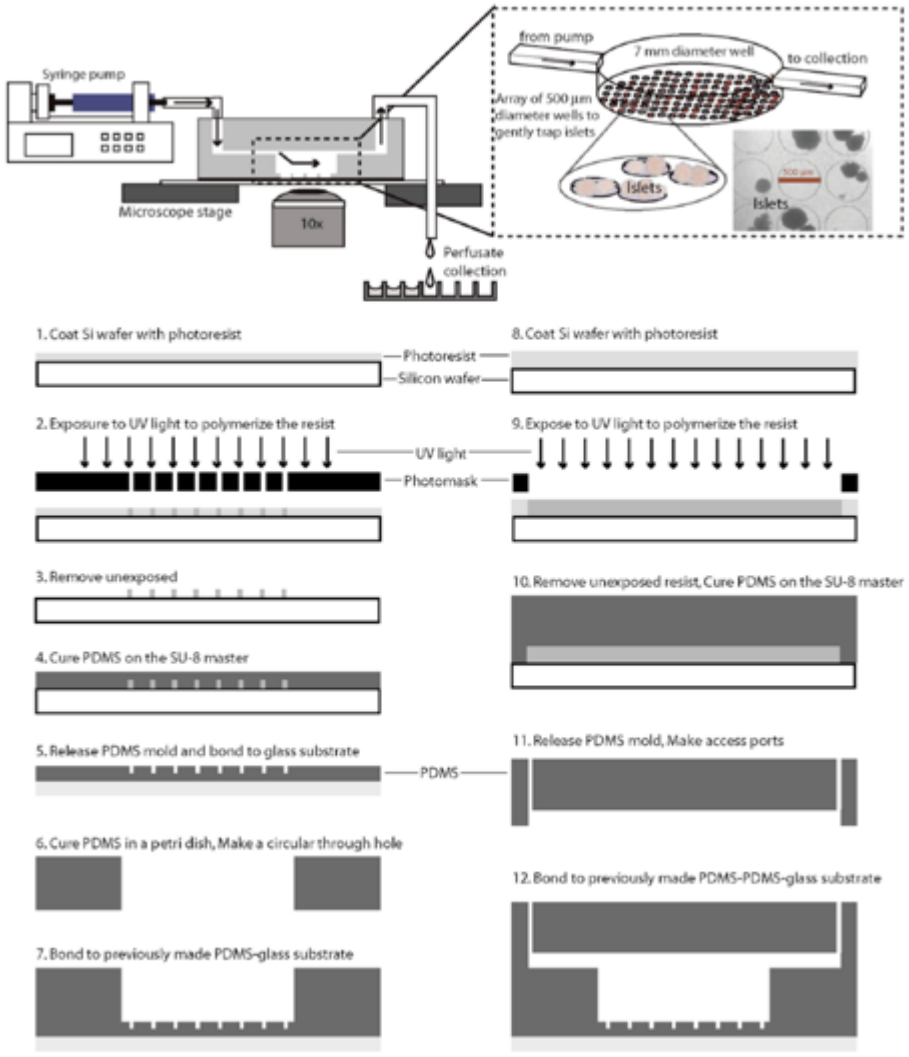

Figure 2.1. Lithography Process. A depiction of the lithography and curing process used by Mohammed et al. (2009)

The microfluidic device designed for this experiment is comprised of three layers: 1) One containing microwells (500 µm in diameter and 150 µm in depth) [Figure. 2.3 i) & ii)], 2) Middle layer containing the microchannel (measuring 19 mm x 2 mm x 250 µm in length, width and depth respectively) and the reservoir cutout (7 mm in diameter and 5 mm in depth) and 3) the transparent layer that covers the first two layers. Layer 1 contains tiny microwells that immobilize the islets

[Figure. 2.3. iii)] and maximize the islet surface area exposure to the perfused liquid [Mohammed et al. 2009] [Figure. 2.3 iv)]. The flow rate of liquid through the perifusion chamber is decided such that the buildup of insulin in the chamber is not allowed to occur (Mohammed et al. 2009) and is below the maximum rates above which considerable shear to the islets would begin to occur. The flow rate of perfused liquid employed throughout this experiment is 0.5 ml/min, though an even larger flow rate of 1 ml/min is still permissible. The specific designs for Layer 1 and Layer 2 are first drawn and designed using AutoCAD [Figure.2.2]. The photomasks for the lithography process were pre-prepared from the AUTOCAD designs using a Laser Writer.

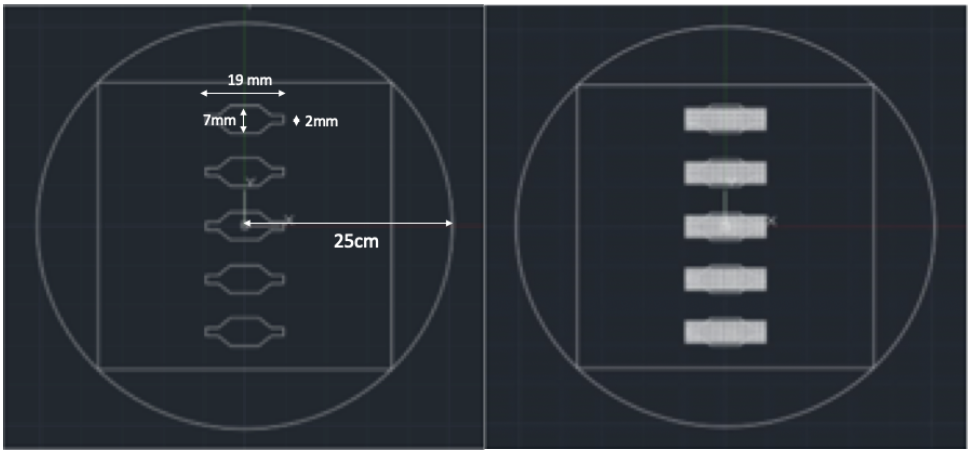

Figure 2.2. AutoCAD Drawings. AutoCAD drawings used to make the photomasks

We then proceeded to spin coat the silicon wafer with the photoresist of choice - SU-8 2050 which was capable of producing the range of thickness dimensions (*Elveflow*) as per our requirement. The coated wafers would then undergo baking cycles on hot plates before and after being exposed to UV light at different energies before leaching away the soluble, unexposed portions of the developed photoresist pattern to leave the patterned masters which would subsequently act as reverse molds for the fabrication of the microfluidic device layers. The baking cycle prior to UV

exposure aims to remove the solvent from the photoresist, thereby solidifying it to an extent, while the post exposure baking (PEB) is to sustain the photoactive reaction started in the photoresist due to UV exposure (*Microchem*). After PEB, the soluble portions of the photoresist were washed away using SU-8 developer solution (1-methoxy-2-propanol acetate) and then air-dried to produce the finished silicon wafers containing the required pattern masters for subsequent device fabrication.

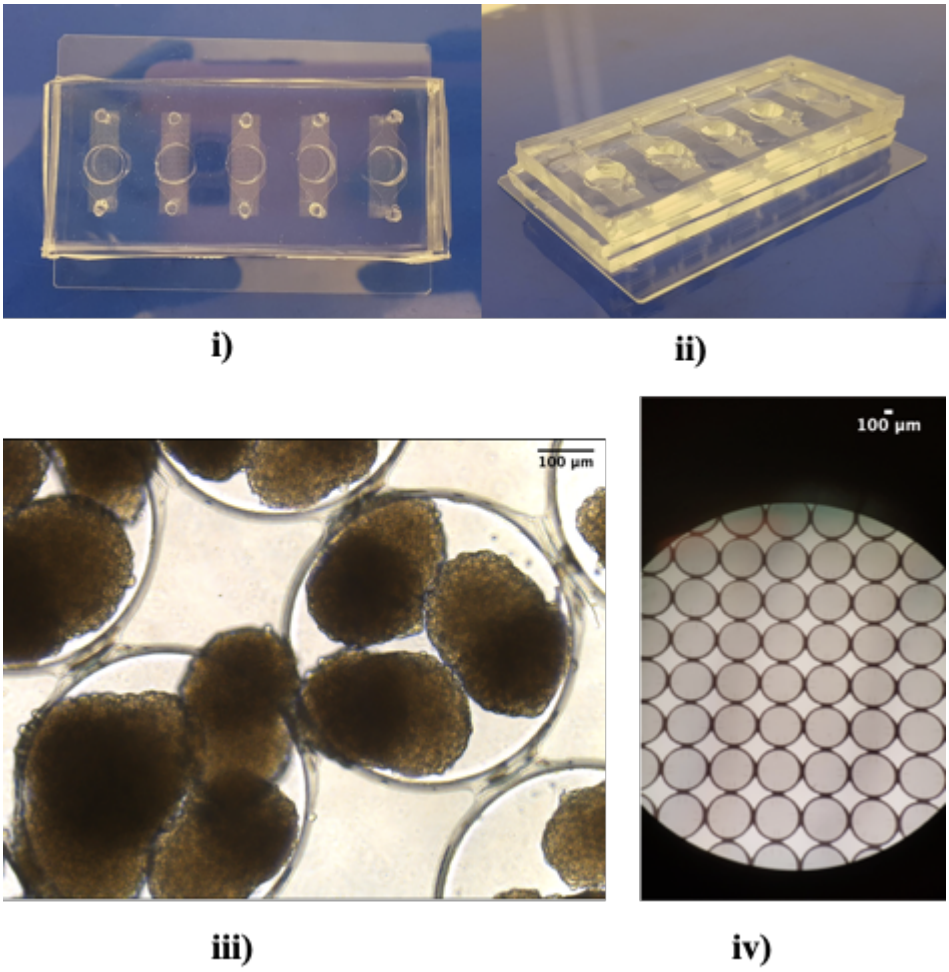

Figure 2.3. Device and Microwell Design. i) & ii) - Images of the finished microfluidic device; iii) Immobilized SCD β cells in Microfluidic device; iv) Microwell design in Layer 1.

2.2. Materials and Methods

2.2.1. AutoCAD files and Laser Writing

The photomasks for Layer 1 and Layer 2 were designed using AutoCAD 2018 software. Designs for both layers were modeled after 50mm diameter sized wafers [Figure. 2.2]. Design files were then used to direct the patterns drawn on the photomask substrates by the Laser Writer to generate the photolithographic masks for selective photoresist exposure.

2.2.2. Spin-Coating, Preliminary Baking Cycles and Photo-Exposure

Layer 1:

Photoresist SU8 - 2050 was applied on a silicon wafer of diameter 50 mm and spin coated at 1300 RPM for 35 seconds. The coated wafer was then baked on a hot plate for 5 minutes at 65 ℃ and then for a longer duration of 30 minutes at 95 ℃. After baking, the coated wafer was placed in a Mask Aligner where the photomask prepared earlier through Laser Writing is mounted in the Aligner. The wafer was then exposed to UV light at an exposure energy of 290 mJ/cm^2 for 3 minutes. The mask and wafer were removed, and the exposed wafer was baked (post exposure baking) for 5 minutes at 65 ℃ and then for 45 minutes at 95 ℃ before being immersed in and treated with SU-8 developer solution with agitation for about 30 minutes. The developed wafer was then rinsed with isopropanol and water and air dried.

Layer 2:

SImilar steps were followed for Layer 2, The Photoresist SU8-2050 was spin coated at 500 RPM for 35 seconds and then soft baked at 65 ℃ for 7 minutes, followed by baking at 95 ℃ for 5 minutes.

The coated wafer was then exposed to UV light at an exposure energy of 385 mJ/cm^2 before undergoing post exposure baking at 65 ℃ for 5 minutes and 95 ℃ baking for 15 minutes. The baked wafer was then treated with SU8 developer solution for about 30 minutes and then rinsed with isopropanol and water. The finished and developed wafer was then air dried.

2.2.3. Polydimethylsiloxane (PDMS) Curing Step and Device Preparation

To fabricate the microfluidic device, 30 g of Sylgard 184 base elastomer was mixed with 3 g of Sylgard 184 elastomer curing agent for a mixing ratio of 10:1 separately in petridishes containing the patterned wafers for Layer 1 and Layer 2 and an empty petridish for Layer 3. The mixture was vigorously stirred until bubbles can be seen. The curing mixture was then deaerated in a vacuum desiccator for long enough until all the bubbles in the mixture disappear. Each of the petridishes are then cured in an oven overnight at ~70 ℃. After curing, using scalpels, the patterned polymer was shaped and removed from the petridishes and inlet holes for Layer 3 and the reservoir hole for Layer 2 was punched out using hole-punches. The polymer slabs and a glass slide (to stick the layers) were then immersed in 70% ethanol and sonicated in a water bath for 20 minutes, to disinfect and remove impurities. As a final step, in order to bond the layers together along with the slide, the slabs were exposed to UV ozone plasma in an Asher/Plasma Cleaner for 30 seconds at 100W with the surfaces to be bonded being exposed. The layers and the glass slide were then aligned and firmly pressed together to complete the process of device fabrication.

2.3. Summary and Conclusion

Here we have recreated and designed a novel microfluidic device for the study and analysis of immobilized pancreatic islet activity. PDMS, specifically Sylgard 184 elastomer, is of choice for this device, owing to its inert and biocompatible properties. Sylgard 184 is a commercially available PDMS elastomer which is commonly used in several biological studies in tandem with applications such as producing elastomers with tunable stiffness (Palchesko et al. 2012). In order to fabricate a functional PDMS microfluidic device, the steps involved began with the fabrication of the masters or the mold for the elastomer to form over and take shape, the former being prepared through the process of negative photolithography using SU8- 2050 as the photoresist. After curing, cleaning and bonding the PDMS layers, the device is then prepared and ready to be used for pancreatic β cell functional studies.

The presence of microwells in the prepared device would be vital for containing cells and reducing possible shear damage, while the device as a whole would help orchestrate dynamic perfusion insulin activity studies in response to step changes in glucose concentration, intended to emulate in vivo conditions. Since the device itself is made of transparent materials, this would allow for further easier and convenient analyses of islet cells using imaging. The photolithographic method of producing microfluidic devices is one of the more conventional methods, it is limited in the sense that it requires cleanroom fabrication and is time consuming and expensive. Several new methods of producing such microfluidic devices have become more preferable, including such as 3D printing, injection replica molding approaches, polymer laminates and other methods of nanofabrication (Gale et al. 2018).

All of these approaches make fabricating microfluidic devices much easier, thereby steadily increasing the preference to design and employ them for screening and staging multiple experiments and microenvironmental conditions. With regard to this experiment, the device is ready to be used after perfusing 70% ethanol and milliQ water to disinfect and clean the working reactor system confined within the device, after which we proceeded to the next steps of loading the device with islet cells and perfusing with low and high concentrations of glucose solution and studying the subsequent insulin activity.

Chapter 3

Perifusional Analysis with Glucose

3.1. Introduction and Results

Through photolithography and elastomer curing techniques, we have designed and fabricated a microfluidic perifusional device. We first proceeded to test the glucose switching action of the microfluidic device, to test the stability of the glucose concentration profile vital for producing a nearly stable insulin secretion profile during the next study of islet activity. The setup for studying glucose switching has been illustrated in Figure. 3.1.i). It comprised of dual syringe pumps capable of producing uniform flow rates of glucose solution, two large capacity syringes containing 2mM and 20mM glucose solutions, mounted on these pumps with tubing to a Y connector, the common outlet of which was connected to the inlet of the microfluidic system. The outlet of the system dispensed glucose samples at intervals of every 2 minutes and concentrations of glucose were measured using Wako glucose assay, the results of which are illustrated in Figure. 3.1.ii). The low glucose region appears fairly stable until the glucose switch performed at the end of 8 minutes, causing a spike in glucose concentration at the end of 10 minutes [Figure. 3.1.ii)], constituting a step change in glucose concentration, before stabilizing at high glucose. These results help establish the fast glucose switching action of the microfluidic device, allowing us to proceed further with using the device with cells to study insulin release activity.

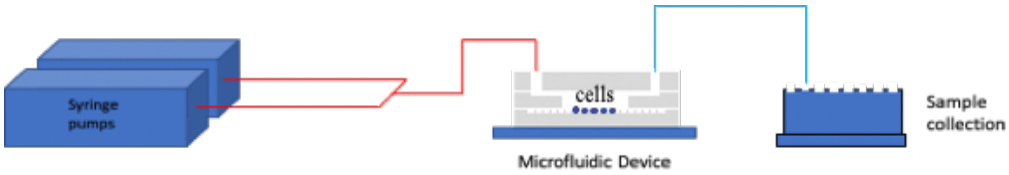

i)

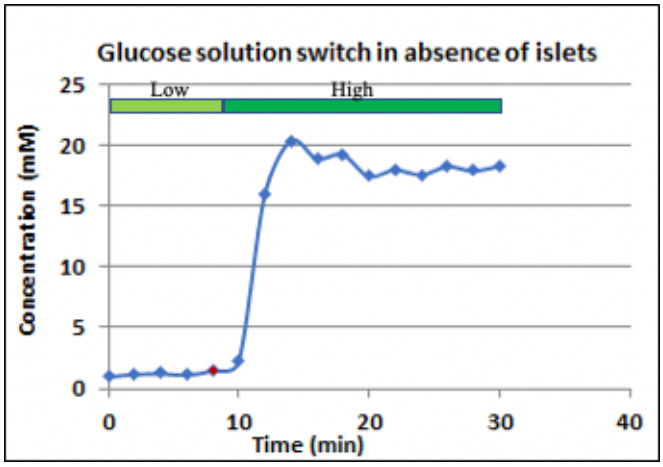

ii)

Figure 3.1. Experiment Setup and Glucose Switching. i) An illustration of the microfluidic perifusion setup used; ii) Glucose switching from 2mM to 20mM at the end of the 8th minute - immediate step change observed

We next proceed to assess the efficacy of the device in providing a suitable environment for human islets and stem cell-derived β cells to function normally under low glucose conditions and in a temperature-controlled environment at body temperature (37 ℃). The setup we used to study low glucose is illustrated in Figure. 3.1.i), comprising of one syringe pump producing a flow rate of 30 mL/h or 0.5 mL/min of low glucose solution. The device was kept temperature controlled at 37 ℃ on a hot plate, with most of the tubing immersed in a water bath at the same temperature. Human insulin and KRB buffer samples were collected from the outlet tubing of the device over intervals of 20 minutes. The samples collected were used to quantify the insulin content using Insulin ELISA.

Before running the experiment, KRB buffer and low glucose (2mM) in KRB solutions were prepared ahead of the experiment and 20-30 islet clusters of SC β cells were loaded into the main perifusional chamber or reservoir of the microfluidic device, ensuring that they were immobilized and did not move even through slight agitation [Figure. 2.3 iii)]. SC β cells were perfused with low glucose KRB solution (2mM) for a total experimental runtime of 110 minutes. After 50 minutes from first being exposed to the low glucose solution, the cells completely stabilize in insulin release activity [Figure. 3.2.], showing their adaptation to their microenvironmental conditions. Furthermore, they show a stable insulin release profile until the end of perifusion runtime. The initial spike in insulin release was expected, owing to their fast insulin release action in response to the new glucose stimulus. These results show that the microfluidic device provided a suitable microenvironment for the study of islet cells and islet activity, without presenting the cells with any mechanical or any other technical perturbation.

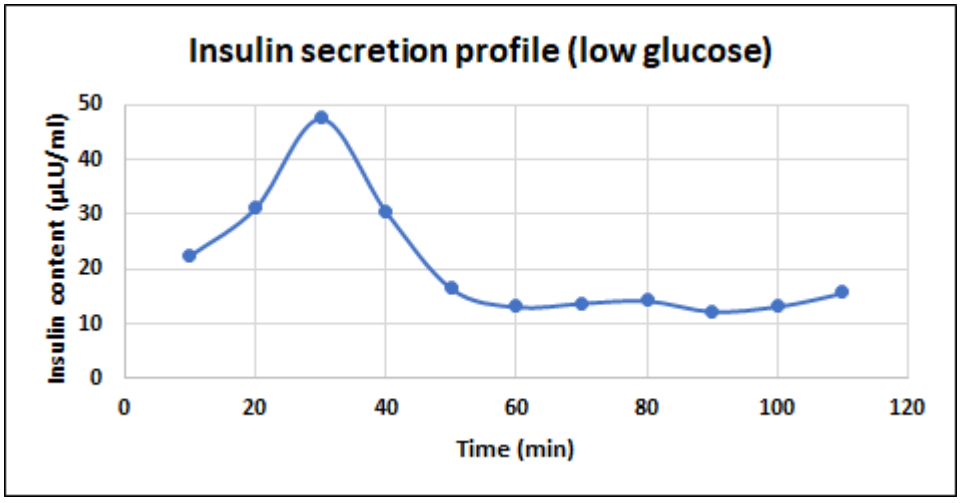

Figure 3.2. Low Glucose Perifusion. Insulin secretion profile under low glucose conditions: near stable profile observed after a duration of 50 minutes.

Finally, we expanded the experiment further to study insulin release activity of human islets in the presence of step change in glucose concentration - from 2 mM to 20 mM. Our setup for the experiment comprised of two syringe pumps mounted with 60mL syringes filled with low and high concentrations (2 mM and 20 mM, respectively) of glucose solutions, similarly configured as that of the glucose switching experiment [Figure. 3.1.i)]. Insulin contained in KRB samples were collected every two minutes. The loaded ~5-10 islets in the device were first perfused with low glucose for a total of 50 minutes to obtain a stable low glucose insulin release profile before switching to high glucose for 20 minutes and once again back to low glucose for 10 minutes. The insulin release profile obtained [Figure. 3.3.] showed slightly undetectable insulin concentration at low glucose due to very few islets used, but still recorded a sharp peak in insulin release (first phase) at the point of switching glucose solutions, followed by a more stable (with respect to time) second phase of insulin secretion, confirming the same results obtained with previously employed methods of perifusional analysis. Hence, here we were able to demonstrate the efficacy of a microfluidic device in eliciting a insulin release response for a step change in glucose concentration. We were also able to study the biphasic response in insulin secretion using said device, in a manner similar to other methods of perifusion.

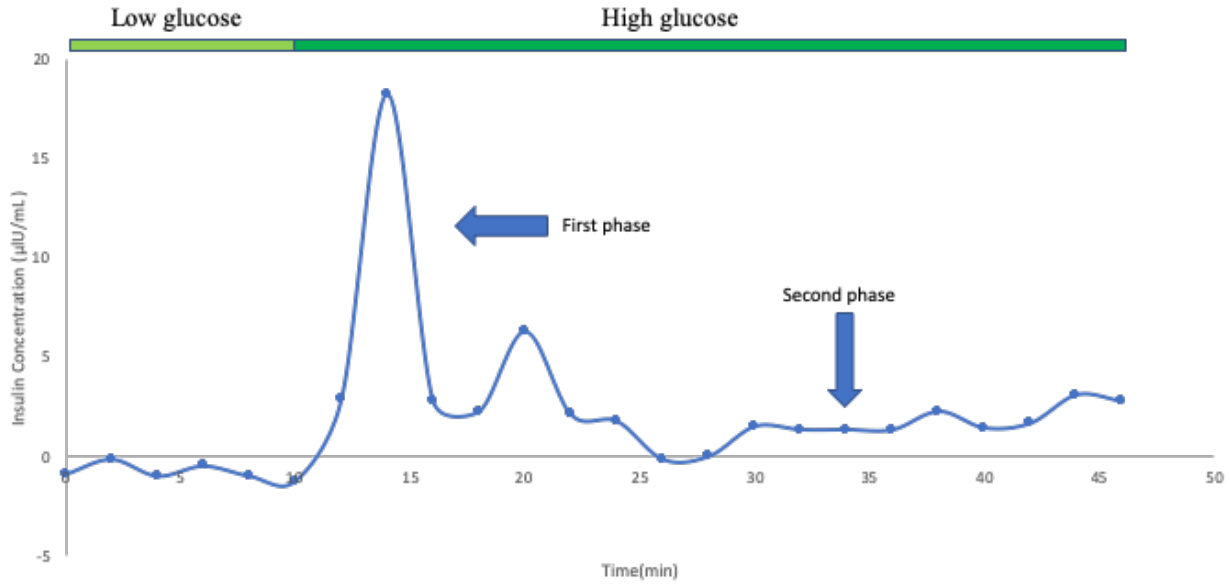

Figure 3.3. Glucose Step Experiment. Absorbance corresponding to concentration of insulin versus time. Biphasic behavior of insulin secretion is observed upon step change in glucose concentration from 2mM to 20mM at the end of 10 minutes.

3.2. Materials and Methods

3.2.1. Preparation of KRB Buffer, low glucose and high glucose solutions for perifusion

KRB Buffer (250 mL) for perifusional analysis was prepared using the composition in Table 3.1. BSA was used to prevent the adherence of insulin to the walls of the device (Adewola et al. 2010). The solution was then brought to a pH of 7.4 using NaOH. For 2 mM (low) glucose solution, 0.018 g of alpha-D-glucose was made up to 50 mL using prepared KRB Buffer. For 20 mM glucose solution, 0.18 g of alpha - D- glucose was made up to 50mL using prepared KRB Buffer.

Components	Quantity
milliQ water	229.1mL
NaCl	12.8mL
HEPES buffer	2.5mL
Na_2HPO_4	2.5mL
$MgSO_4$	0.3mL
KCl	0.625mL
$CaCl_2$	0.675mL
$NaHCO_3$	0.3mL
BSA	0.25g

Table 3.1. KRB Buffer Components. Components comprising 250 mL of Krebs-Ringer Buffer.

3.2.2. Estimation of insulin content in samples using Insulin ELISA

25 µL of samples along with standard solutions were pipetted out into a 96 well plate, and 100 µL of secondary antibody was added to all of the wells using a multichannel pipette. The plate was then covered and kept in a shaker for an hour. After shaking, the media was dumped out and the wells were washed with human ELISA wash buffer 6 times and media repeatedly dumped out. The plate was then made to dry on a napkin before adding 100 µL of TMB substrate to the wells using a multichannel pipette. The plate was then kept on a shaker for 15 more minutes, after which 100 µL of stop solution was immediately added to stop the reaction. The plate was then read in a plate reader with light wavelength at 450nm. This way a standard curve was obtained whose equation was used to calculate the insulin concentration over the concerned period of time.

3.3. Summary and Conclusion

Here, we have demonstrated how the fabricated microfluidic device through photolithography and PDMS curing steps, could be used as an alternative to traditional methods of perifusion. We have shown that the device is capable of fast glucose switching action - ~2 minutes interval in response change corresponding to a flow rate of 0.5 mL/min. This quick glucose switching action is ideal for the study of glucose associated activity in islets, such as insulin secretion. Islets show a swift response to changes in glucose concentration, thereby making it essential for the change in glucose concentration to happen in a quick manner to produce an accurate insight into the insulin release activity of these cells. To put this forth in a practical sense, we showed how the cells produced a stable insulin release profile after a short while, in the presence of low glucose flow, further emphasizing on the compatibility of the cells with the device, and showing that they are merely immobilized in the microwells and not bonded to the substrate in any way.

We could also demonstrate how the cells could respond positively in the presence of a glucose step gradient from 2 mM (low) to 20 mM (high) concentrations. A two phase insulin secretion profile as expected was observed - with the first phase appearing as an abrupt spike in the secretion of insulin with respect to time and the second phase appearing as a stable secretion of insulin with respect to time, before low glucose was once again made to flow through the device. This way, we have put forth and re-demonstrated the utility and compatibility of our microfluidic device for the study and perfusional analysis of pancreatic human islet and stem cell derived pancreatic β cells. To explore the further functionality and advantage of using such a device, we shall proceed to imaging experiments with human islets and stem cell derived β cells to study calcium ion fluorescence intensity profile in tandem with insulin release activity.

Chapter 4

Calcium Fluorescence Imaging of HI and SCD B Cells

4.1. Introduction and Results

Having demonstrated the use of the microfluidic device as a system capable of mimicking traditional perifusional systems in terms of assessing insulin release activity in response to glucose stimulation, we motioned towards the imaging aspect of our experiment, utilizing one of the main advantages of using a transparent microfluidics device for the purpose. Through calcium fluorescence imaging and perifusional analysis, we first aimed to obtain the fluorescence intensity profile equivalent to calcium ion activity in the cells upon glucose stimulation and directly comparing it with the insulin secretion profile, estimated through the insulin ELISA assay. During the process of insulin granule exocytosis upon glucose stimulation, the influx of calcium ions is expected to occur, subsequently binding with the Fluo-4 AM fluorophore present in the cells to produce fluorescence. We expect to see a larger intensity of fluorescence corresponding to a larger concentration of glucose stimulus. To confirm the responsivity of these cells to the low and high glucose concentrations, we introduce a KCl control step after the high glucose regime, where we would expect to see a drastic increase in the fluorescence intensity and insulin owing to KCl depolarization of the islets leading to a large influx of calcium ions and a simultaneously large release of insulin.

We began our experiment by preparing perifusing fluids - namely low glucose (2 mM) glucose solution in KRB (Krebs-Ringer Buffer), high glucose (20 mM) KRB and 30 mM KCl in KRB

solutions. ~ 35 clusters of cadaveric donors pancreatic (HI) β cells were stained with the fluorescent dye Fluo-4 AM through a series of washing steps with low glucose Krebs-Ringer Buffer. 10 mL of low glucose KRB was perifused into the microfluidic device after cleaning with milliQ water and 70% ethanol. The cells were then loaded into the device, which was then set up in as shown in Figure. 4.1.i), with the tubing and device heated to 37 ℃. The device was heated on a thermal stage below a fluorescence macroscope. The cells were then perfused with low glucose for 20 minutes to equilibrate the cells and marginally stabilize low glucose insulin activity. Readings were then taken in the low glucose regime for 10 minutes before switching into high glucose for 15 minutes and finally with 30 mM KCl for another 15 minutes. Images were captured in a time series of a total of 200 cycles with acquisition occurring every 15 seconds. The perfusate was simultaneously collected over intervals of every 1 minute. The time series images acquired were analyzed using ImageJ/Fiji software, and a fluorescence intensity profile was generated (Figure. 4.2. shows the fluorescence intensity profiles for all of the islets imaged). Every three perfusate samples (worth 3 minutes in total) were acquired at a time were mixed to form one sample of many and analyzed using Insulin ELISA to obtain a insulin secretion profile which was then directly compared to the fluorescence intensity profile of an islet with the most positive (with respect to the expected data acquired) response to glucose and KCl as illustrated in Figure. 4.3.

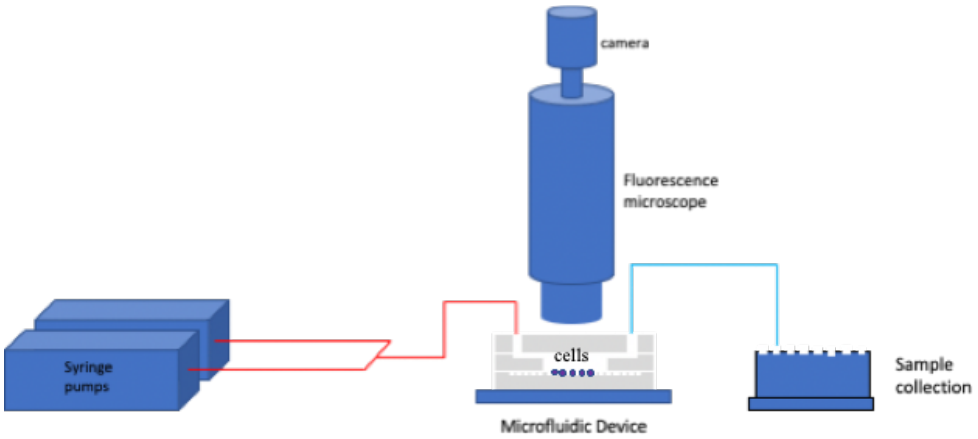

i)

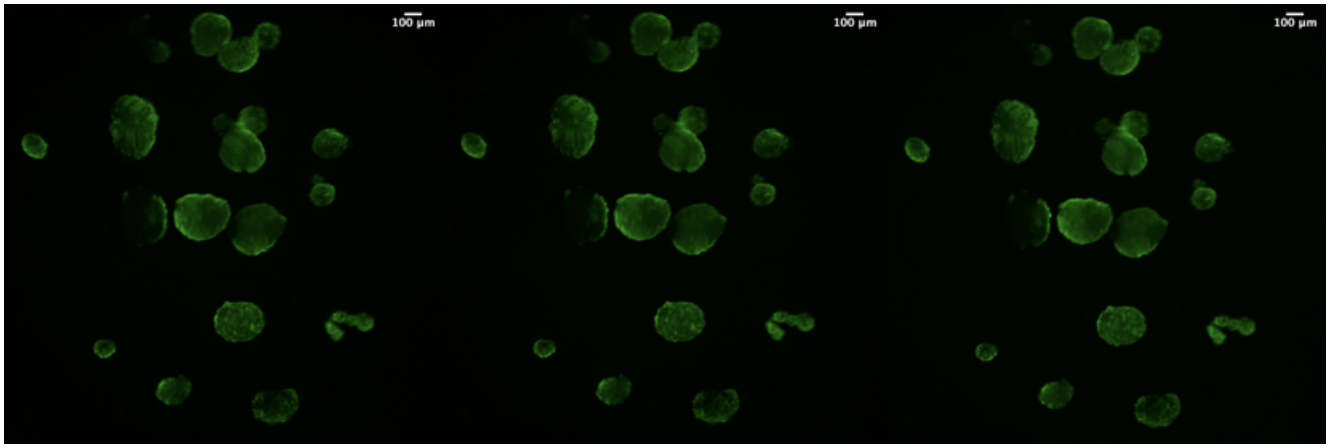

ii)

Figure 4.1. Experiment Setup and Fluorescence Images. i) Illustration of the imaging and perifusion setup; ii) HI clusters stained with 20 µM fluo-4 AM exhibiting increasing intensities (from left to right) from low glucose (t = 9.25 min), high glucose (t = 20.5 min) and KCl (t = 29 min) stimulation

We categorized the individual islet fluorescence responses as follows: i) Positive responses, which showed a near-stable low glucose response prior to spiking after a high glucose switch (t = 10 min) and spiking even further in response to the KCl control (t = 25 min), as expected; ii) Uncertain

responses, most of which had not stabilised in fluorescence intensity during the low glucose regime, and hence were uncertain with respect to their high glucose response, but nevertheless positively responding to the KCl control; iii) Negative responses, both of which did not respond to high glucose and the KCl control entirely, or to the degree expected [Figure. 4.2]. The fraction of success, or the number of islet clusters positively responding to high glucose and KCl stimulation with respect to the total number of islet clusters imaged was 6 out of 18 clusters. Directly comparing a positive fluorescence islet response to the insulin secretion profile obtained using the ELISA [Figure. 4.3] first showed a very small spike in insulin concentration (first phase) after t = 10 min (High glucose stimulation) corresponding a larger spike in fluorescence intensity, followed by a very weak second phase of insulin secretion correlated with a dip in fluorescence intensity until t = 25 min (KCl control stimulation). After this point, both profiles showed a large increase in calcium ion activity as well as insulin concentration. This spike in fluorescence intensity during KCl control stimulation confirmed that most of the cells were functional and barely glucose-responsive, corroborated by the increased insulin secretion during high glucose and KCl stimulation, albeit to a much lower degree than what was originally expected.

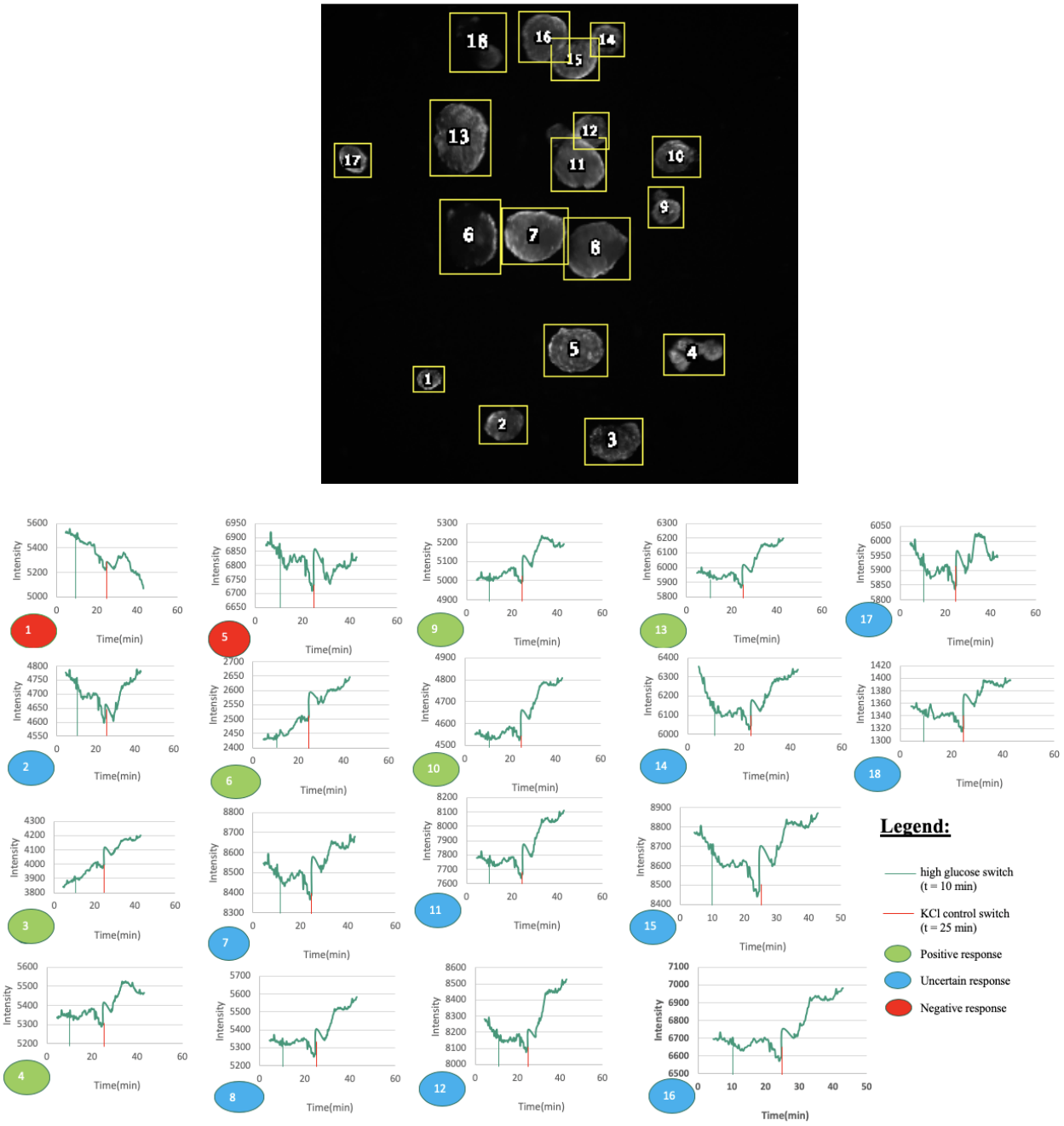

Figure 4.2. ROI's and HI Analysis. Fluorescence intensity profiles of all human islets obtained with corresponding ROI's

Hence, these results demonstrate that through the use of dynamic microfluidic perifusion and simultaneous dynamic calcium fluorescence imaging, we could show and obtain a direct relationship between Ca^{2+} activity within the Human islets and insulin release activity. Furthermore, from the data obtained, we made an additional observation that the resolution of measured data acquired using image acquisition every 15 seconds was evidently higher than that obtained by ELISA, where samples were collected on an average of every 3 minutes [Figure. 4.3].

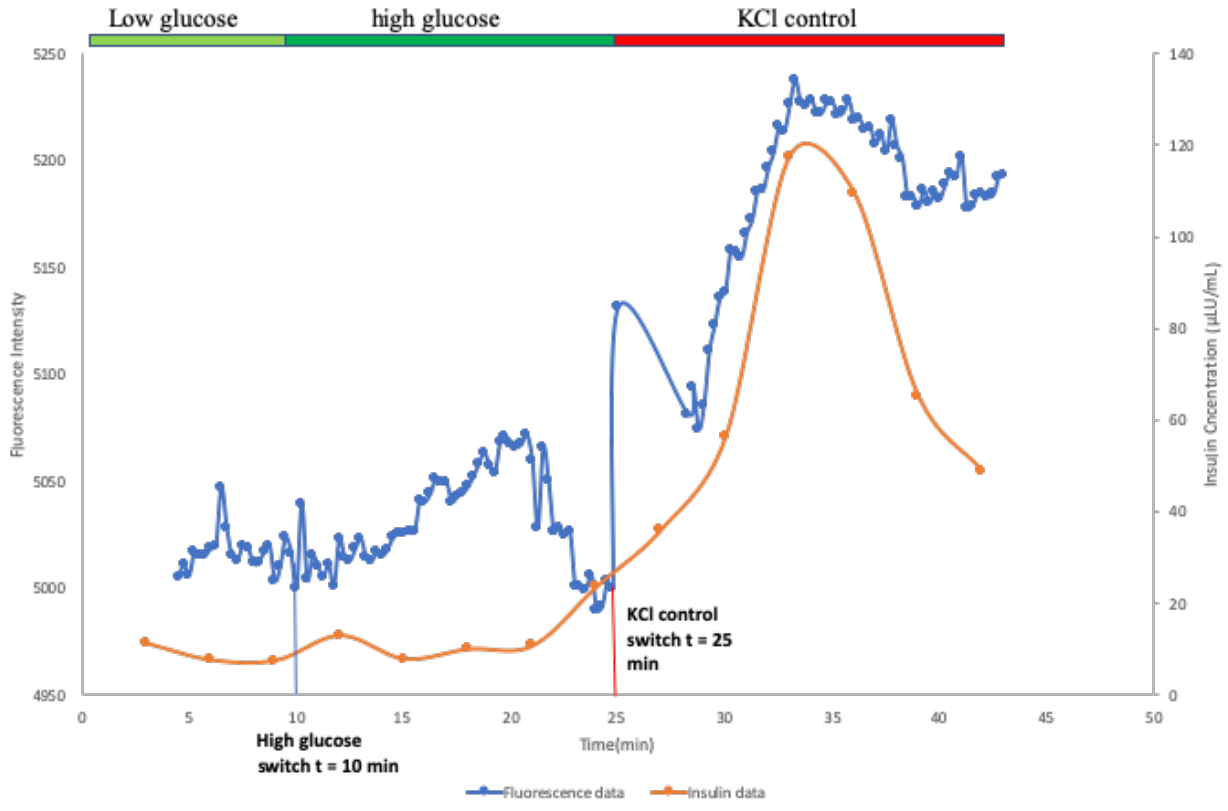

Figure 4.3. Comparison of Fluorescence Intensity with Insulin-1. Insulin secretion profile for Human islets compared to a positive calcium fluorescence islet response (high glucose induced at t = 10 min and KCl at t = 25 min)

We then proceeded to take the step further to assess the insulin release and Ca^{2+} activity of the SCD β cells synthesized and differentiated by the Millman Lab. We first aimed to obtain fluorescence response profiles for all islets imaged, directly comparing them to their corresponding insulin secretion profile obtained using the insulin ELISA, before comparing and contrasting the calcium fluorescence and insulin secretion data of these cells with that previously obtained using the Human islets. Around 25 islet clusters of SCD β cells were stained using the similar Fluo-4 AM protocol and loaded onto the microfluidic device after pretreating and pre-equilibrating the latter with milliQ, 70% ethanol and low glucose KRB. The cells were then equilibrated with low glucose KRB for 20 minutes before data was collected for 8 minutes in the (2 mM) low glucose region. At the end of 8 minutes, high glucose (20 mM) was switched in for 15 minutes, followed by KCl (30 mM) control solution for 10 minutes. Perfusate samples were once again collected every 1 minute with images acquiesced every 15 seconds for a total of 200 cycles. The images obtained were also analysed similarly with the use of ImageJ/Fiji software [Figure 4.5], and every 3 samples (every 3 minutes) were assayed using ELISA.

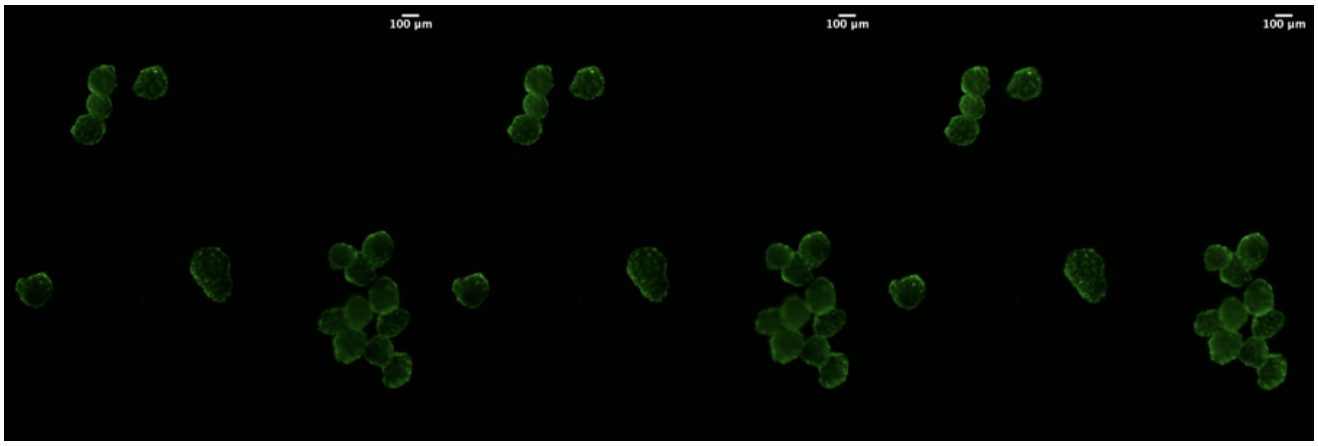

Figure 4.4. SCD β Cell Fluorescence Images. Images of SCD β clusters stained with 20 µM fluo-4 AM exhibiting increasing intensities (left to right) corresponding to low glucose stimulation at t = 7.75 min, high glucose stimulation at 9.25 min and KCl stimulation at t = 30.5 min respectively.

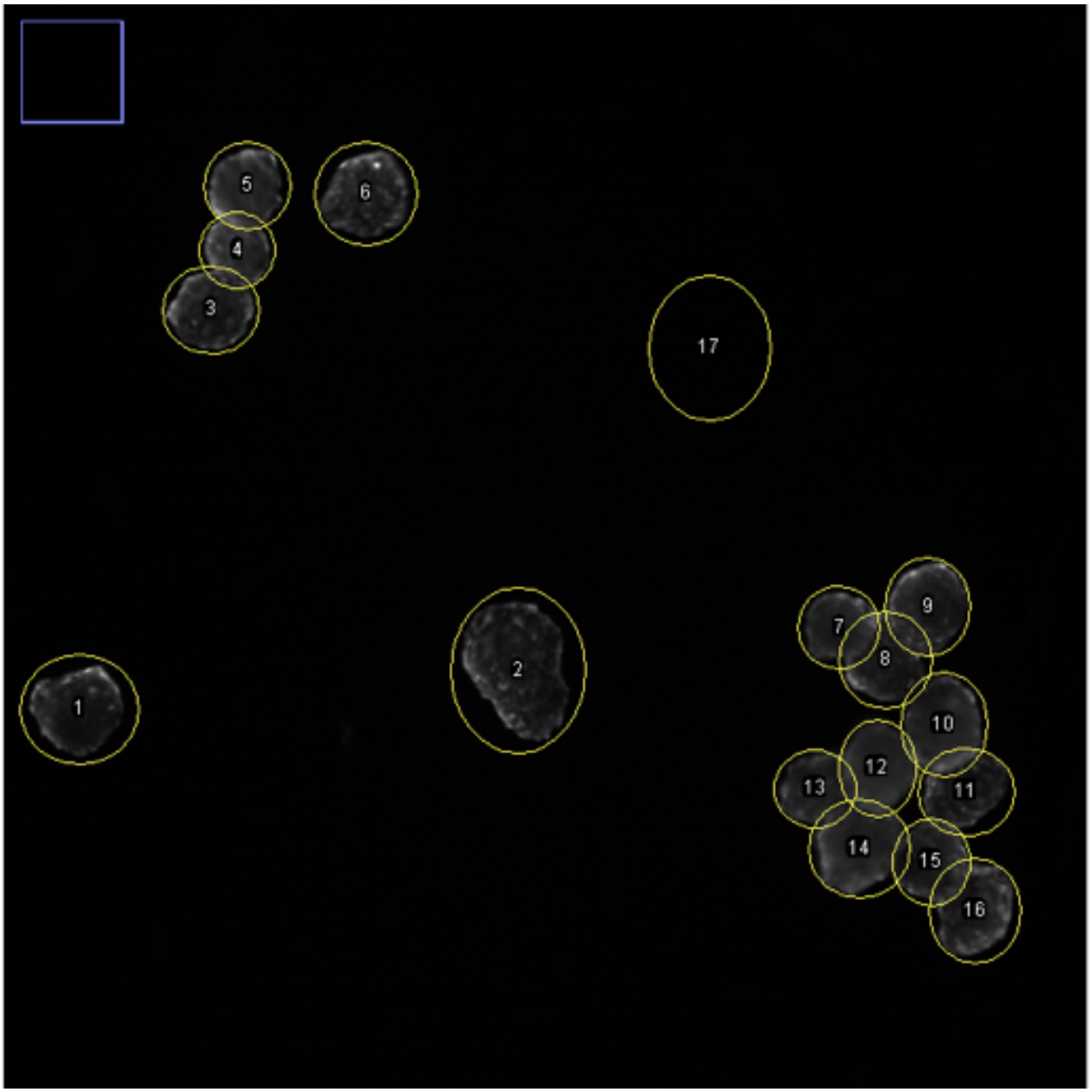

Figure 4.5. ROI Analysis of SCD β cells-1. Regions of Interest (ROIs) used with the analysis of SCD β cells

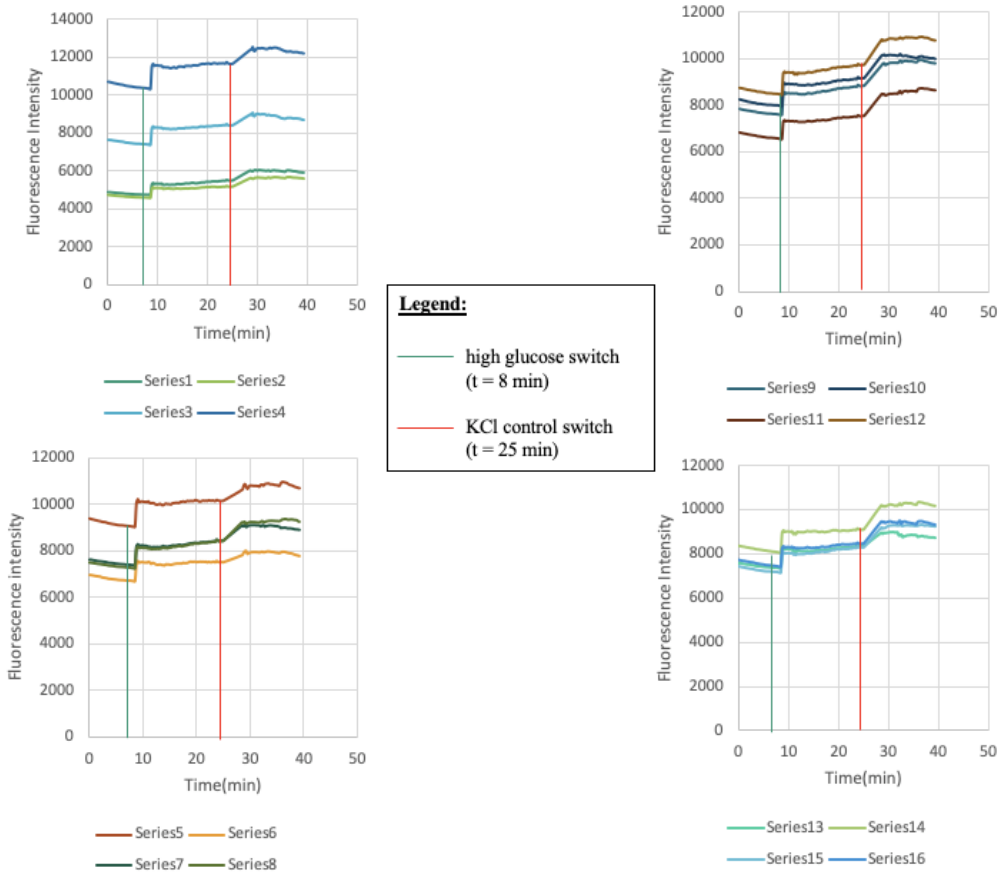

Figure 4.6. ROI Analysis of SCD β Cells -2. Fluorescence intensity profiles of all HI islets obtained with corresponding ROI's

The fluorescence intensity profile of all of the islets, as illustrated in Figure. 4.6. showed an abrupt spike in calcium activity after high glucose was switched in (t = 8 min), followed by a marginal to large increase in the fluorescence intensity observed after KCl was introduced to the system at t = 25 min. Hence, the unexpected fraction of success obtained in this case was 16 positive islet responses out of 16 islets, which was scrutinized by directly comparing the fluorescence intensity data with the insulin secretion profile. Both profiles showed a substantial spike in insulin secretion and Ca^{2+} activity at the end 8 minutes [Figure. 4.7]. In this case, the fluorescence intensity remained nearly uniform corresponding to a slowly increasing second phase of insulin secretion up until the

end of 25 minutes, when the KCl was switched in. Thereafter, both profiles exhibited a large increase in Ca^{2+} and insulin secretion activity in response to KCl, out of which, the insulin concentration reached a highly saturated value not within the standard range used with the ELISA [Figure. 4.7]. The fluorescence activity obtained in the KCl control regime confirmed the viability of the SCD β cells analysed, bolstered by the insulin secretion data acquired and compared.

We proceeded to contrast the data obtained from both HI and SCD β cells by directly comparing their fluorescence intensity profiles obtained [Figure. 4.8] As also evident from the fractions of success obtained, we observed a stark contrast in glucose and KCl response in the case of SCD β cells compared to the Human islets, the change in responses of the latter almost completely masking the fluorescence changes obtained using human islets. We could attribute this very large and unexpected difference in responses to various experimental and biological factors concerning this *in vitro* study of comparing HI and SCD β cell activity.

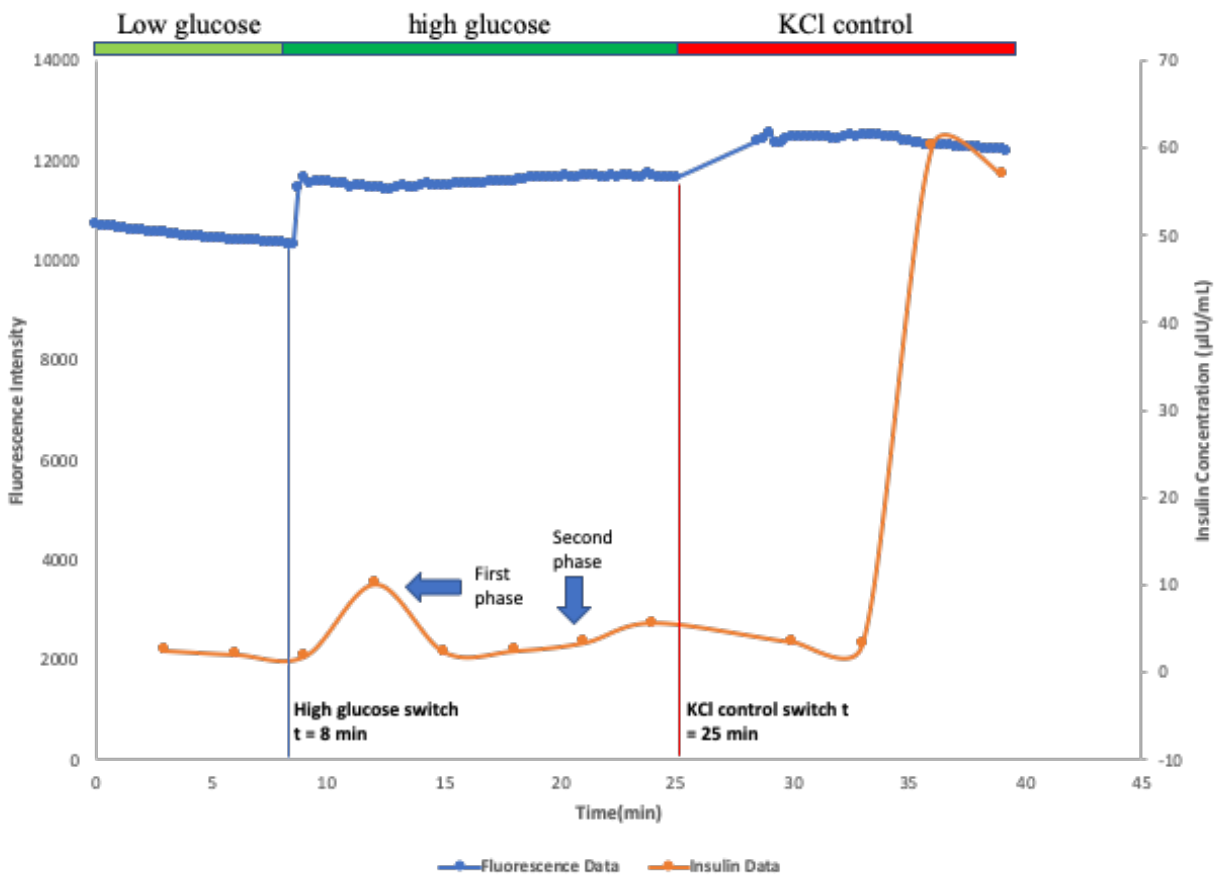

Figure 4.7. Comparison of Fluorescence Intensity with Insulin -2. Insulin secretion profile of SCD β cells with high glucose stimulation at t = 8 min and KCl control stimulation at t = 23 min.

Hence, here we compared and contrasted the glucose-stimulated functional activity of human islets and SCD β cells by dynamically analyzing Ca^{2+} fluorescence islet profiles through imaging, comparing them directly with an equivalently matched insulin secretion profile through the utilization of a versatile microfluidic device bringing about the ability to perform both types of dynamic analyses.

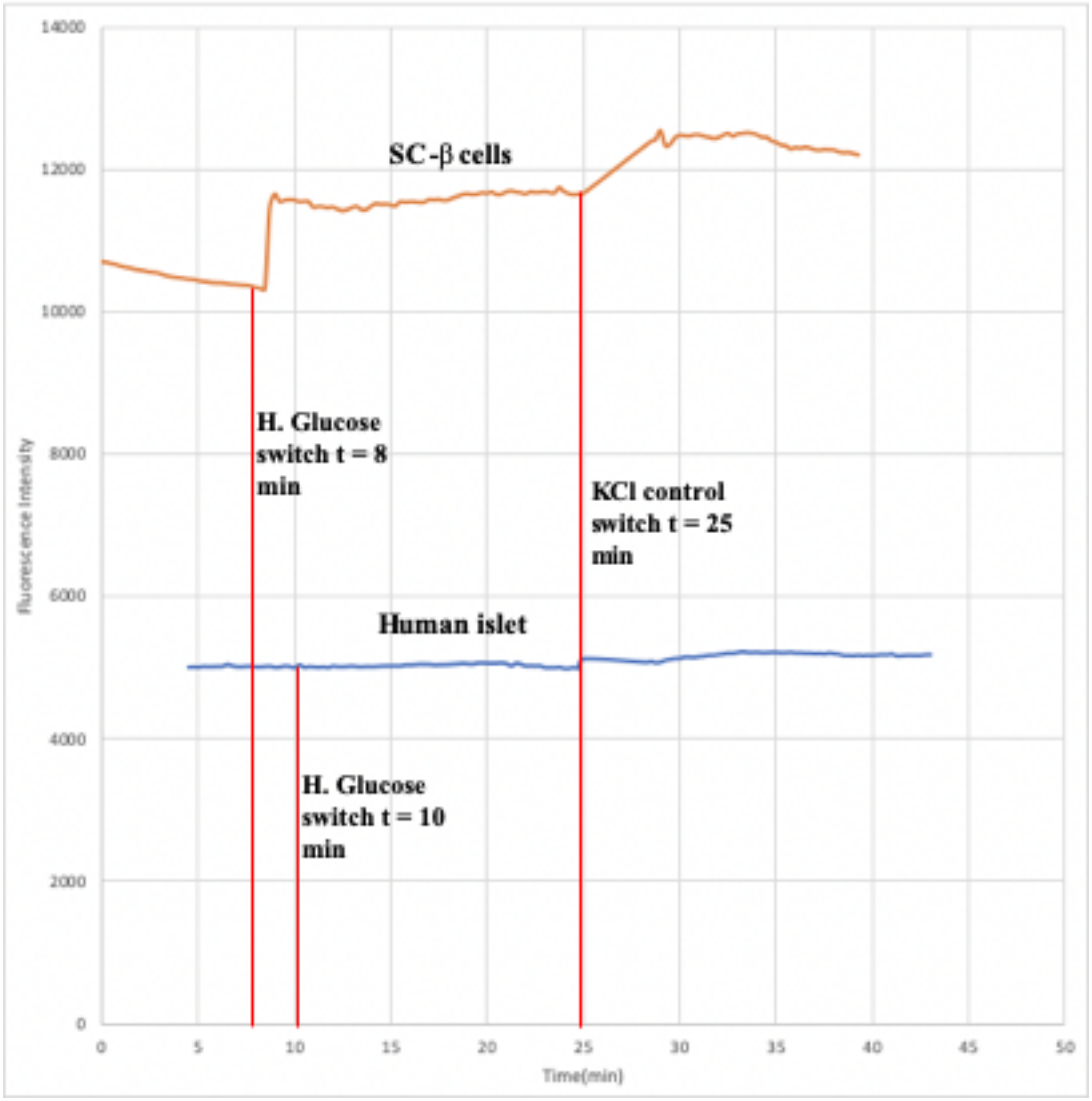

Figure 4.8. Comparison of Fluorescence Data of HI and SCD β Cells. Comparison of HI β cell fluorescence data with SCD β cell fluorescence data shows a much higher glucose and KCl response in the case of SCD β cells as compared to human islets.

4.2. Materials and Methods

4.2.1. Fluo-4 AM Staining Protocol

Fluo-4 AM was obtained from the company ThermoFisher Scientific as 50 μg vials. A 2mM stock of Fluo-4 AM was made by mixing 50 μg of Fluo-4 with 22.8 μL of DMSO (dimethyl sulfoxide). 10 μL of this sample was mixed with 1 mL of low glucose KRB (2mM) to produce a 20μM staining solution. Both HI and SCD β cells were collected in a 1.5mL centrifuge tubes and were first washed twice with 200 μL of low glucose KRB after draining nutrient media. The supernatant was removed after each washing before adding 500 μL of staining solution in the tube. The cells were then incubated in this solution for 45 minutes at body temperature. The supernatant was then removed and the washing steps with low glucose KRB were repeated, leaving 200 μL of low glucose KRB supernatant after the second washing step. The cells were loaded into the microfluidic device for analysis.

4.2.2. Image Analysis using ImageJ/Fiji Software

Images were acquiesced using a Hamamatsu CCD camera used with a Zeiss Axio Zoom V16 Macroscope for fluorescence imaging at 50X magnification. The time series images were present as a stack of multiple images which were analyzed as a hyperstack using ImageJ/Fiji software. They were first corrected for translational movement using the StackReg feature, after which they were analyzed with Regions of Interest (ROI's) for each entire islet cluster, and a fluorescence intensity profile was generated using the data, with background noise subtraction. Plots of the intensity profile were made using Microsoft Excel.

4.3. Summary and Conclusion

Here, we demonstrated studies involving the simultaneous dynamic perifusion and calcium fluorescence imaging of HI and SCD β cells by means of employing a microfluidic device for the purpose. Our first study revolved around applying this analysis towards Human islets, where we were able to directly compare a positive calcium fluorescence intensity profile with the human insulin secretion profile, and found similar changes in magnitude of insulin secretion and fluorescence intensity, with a small spike and steady change in insulin (representing the first and second phases of insulin secretion, respectively) and a transient spike in fluorescence at high glucose (t = 10 min) and more significant increases in both towards the KCl control region. The KCl control was used as an indicator of the responsiveness of the islet β cells, using which we observed that while most of the islets were KCl-responsive, some islets yielded only a small response to the high glucose and a marginal response to the KCl (fraction of success being 6 out of 18 islets imaged), and were categorized accordingly.

The SCD β cells utilized as part of the second study, in contrast, showed more responsiveness, in terms of their steep changes in Ca^{2+} fluorescence upon stimulation with high glucose and KCl. The cells showed a large first phase insulin response in equivalence with an abrupt spike, tailed by stable Ca^{2+} fluorescence behavior upon stimulation with high glucose (t = 8 min), and ultimately showing an even larger increase in fluorescence, equivalently compared to the increase in insulin secretion upon treatment with KCl (t = 25 min). In this case, all of the islets were observed to have responded to the glucose and KCl stimulation, with the fraction of success being 16 out 16 islets imaged. After directly comparing best case fluorescence intensity profiles of both HI and SCD β cells, it could be concluded that Human islets used had reduced viability *in vitro*. This could be attributed to both

experimental and biological reasons such as the high functional variability of these cells from donor to donor depending on reasons such as the cause of death, or could also be attributed to the purification, handling and logistics involved before the cells are procured and ready for analysis. In addition to this, the foreign microenvironment may also have a role to play in reducing viability of these cells due to limited adaptability in artificial nutrient mediums, as well as in the perfusing fluids flowing through the microfluidic environment.

The SCD β cells, in contrast, were evidently more adaptable to *in vitro* conditions, cultured and differentiated in large numbers and were more adapted to artificial nutrient mediums as compared to human islets. This could serve as a possible explanation for their superior performance during this experimental run. While this experiment might have yielded results contrasting with originally anticipated observations, it is still clear that healthy human islets perform better and function in a way necessary to sustain a normal and regulated blood sugar level, which, at the moment, place them above current SCD β cells, in terms of functional capabilities. Perhaps subsequent test runs with different donor islets might demonstrate this. With the current progress of research in this field, it could be possible that in the near future, islet transplantation therapy could be substituted with equivalently functioning SCD β cell treatment, which would serve to eliminate the current gap existing between them, and microfluidic analysis could potentially play a significant role in bridging this gap.

Chapter 5

Future Directions and Possible Improvements

Microfluidics is no doubt a means for efficient assessment of cellular and other biological activity in a variety of research scenarios, owing to their versatility, ability to generate multiple experimental conditions for a single assessment, etc. With regard to our current experiment, we proceeded to fabricate these devices through conventional SU-8 photolithography. This process of fabricating microfluidic devices requires the use of specific facilities like a cleanroom, as well as requires a lot of labor when sophisticated designs of microfluidic devices are involved (Kamei et al. 2015). Specific channel heights and other dimensions as part of a convoluted design of the microfluidic device becomes an arduous task sometimes having the requirement to depend on different kinds of photoresists capable of producing the desired dimensions, as well as a myriad of spin coating or baking conditions which would be required to produce dimensions of different thickness. It is overall a time consuming, expensive and labor-intensive process (Kamei et al. 2015).

It also may not be completely possible to generate the most intricate of designs using photolithography, taking the example of the microwells in the device that we used - The laser writer did not have enough precision to completely separate (a few micrometers distance) each well from the other. These limitations make photolithography an unwise choice to fabricate microfluidic devices where the designs are highly convoluted and/or several devices need to be produced over a short span of time, or even when the required facilities for fabrication are not available. 3D bioprinting of lithography molds for PDMS device fabrication could potentially be an easier, cost-

effective and better solution for the rapid production of PDMS-based microfluidic devices (Kamei et al. 2015). It would be possible this way to construct some of the most complicated and intricate of designs, even those structures that can exceed a height of 1 mm (Kamei et al. 2015), which is not possible with conventional photolithography. Production of these molds using 3D bioprinting also circumvents the necessity to work in a cleanroom or other specific facilities as opposed to photolithography.

The dynamic microfluidic perifusional analysis of islet activity, specifically the study and quantification of insulin released in response to glucose stimulation using insulin ELISA is definitely effective, but comparing it with the resolution of measurement obtained with calcium imaging (a measurement for every 15 seconds), it becomes impractical to use a large number of samples for the ELISA, due to it becoming extremely time-consuming and expensive. A possible future aim in this research could look at the prospect of indirectly determining and quantifying the insulin release activity through dynamic measurement of fluorescence intensity changes in response to calcium ion influx during glucose stimulation. This method of quantification could very well provide a large scale of resolution since every measurement of fluorescence intensity change could correspond to a value of insulin quantity secreted and would serve as an accurate and inexpensive method of insulin quantification as opposed to the Insulin ELISA.

Another research approach which is gaining some attention is the estimation of insulin through luciferase assays. Luciferases are a class of oxidative enzymes that catalyze the reaction of luciferin to oxyluciferin resulting in the emission of light (bio-luminescence) (*Bitesizebio*). The regulatory regions of the genes that express the gene of interest are cloned in an expression vector and the

resulting vector DNA is introduced into the cells. When these cells are made to rupture and are treated with luciferin and other cofactors, it should theoretically lead to the bioluminescence of the oxyluciferin generated due to the luciferase enzymatic activity which can be measured using a luminometer (*Bitesizebio*). Since the luciferase gene is linked to the gene of interest, the intensity of luminescence produced would directly quantify the relative concentration of protein expressed by the gene. The luciferase assay is sensitive, convenient and relatively inexpensive.

An example of application of such an assay for insulin quantification was conducted in this study where *Gaussia* luciferase was inserted into the C-peptide of proinsulin (Burns et al. 2015). Under standard or induced conditions (in the presence of ER toxins, fatty acids or cytokines) the luciferase would be co-secreted with insulin in "close correlation" (Burns et al. 2015), possibly producing bioluminescence with luciferin leading to easy quantification of insulin. Such a method does not involve a perifusional analysis and helps in identifying different pathways of insulin secretion much faster. All of these methods and future research on the assessment and study of islet activity could very well pave the way for the complete treatment and eradication of Type-1 Diabetes.

References

1. Mohammed, J. S. et al. “Microfluidic Device for Multimodal Characterization of Pancreatic Islets” NIH Public Access. *Lab Chip* **141**, 520–529 (2009), doi: 10.1039/b809590f
2. Pagliuca, F. W., Millman, J. R., Gürtler, M., Segel, M., Van Dervort, A., Ryu, J. H., … Melton, D. A. (2014). Generation of functional human pancreatic β cells in vitro. *Cell*, *159*(2), 428–439. https://doi.org/10.1016/j.cell.2014.09.040
3. Type-1 Diabetes Facts (n.d.). Retrieved from https://www.jdrf.org/t1d-resources/about/facts/
4. Hirsch, I. B., Farkas-Hirsch, R., & Skyler, J. S. (1990). Intensive insulin therapy for treatment of type I diabetes. *Diabetes Care*, *13*(12), 1265–1283. https://doi.org/10.2337/diacare.13.12.1265
5. Leibiger, I. B., Leibiger, B., & Berggren, P.-O. (2008). Insulin Signaling in the Pancreatic β-Cell. *Annual Review of Nutrition*, *28*(1), 233–251. https://doi.org/10.1146/annurev.nutr.28.061807.155530
6. Rorsman, P., & Renström, E. (2003). Insulin granule dynamics in pancreatic β cells. *Diabetologia*, *46*(8), 1029–1045. https://doi.org/10.1007/s00125-003-1153-1
7. MacDonald, P. E., Joseph, J. W., & Rorsman, P. (2005). Glucose-sensing mechanisms in pancreatic β-cells. *Philosophical Transactions of the Royal Society B: Biological Sciences*, *360*(1464), 2211–2225. https://doi.org/10.1098/rstb.2005.1762
8. Wang, Z., & Thurmond, D. C. (2009). Mechanisms of biphasic insulin-granule exocytosis - roles of the cytoskeleton, small GTPases and SNARE proteins. *Journal of Cell Science*, *122*(7), 893–903. https://doi.org/10.1242/jcs.034355
9. Popa, S., & Mot, M. (2013). B-Cell Function and Failure in Type 2 Diabetes. *Type 2 Diabetes*. https://doi.org/10.5772/56467
10. “Microfluidics and Microfluidic Devices: A Review” (n.d.). Retrieved from https://www.elveflow.com/microfluidic-tutorials/microfluidic-reviews-and-tutorials/microfluidics/

11. Yin, B. S., Li, M., Liu, B. M., Wang, S. Y., & Zhang, W. G. (2015). An integrated microfluidic device for screening the effective concentration of locally applied tacrolimus for peripheral nerve regeneration. *Experimental and Therapeutic Medicine*, *9*(1), 154–158. https://doi.org/10.3892/etm.2014.2082
12. Adewola, A.F. *et al.* A Multi-Parametric Islet Perifusion System within a Microfluidic Perifusion Device. *J. Vis. Exp.* 6–7 (2010). doi:10.3791/1649
13. Perifusion System (n.d.). Retrieved from http://www.biorep.com/product/perifusion-system/
14. Hassan, M., & Klaunberg, B. A. (2004). *Comparative Medicine Overview Biomedical Applications of Fluorescence Imaging In Vivo*. *54*(6), 635–644. Retrieved from http://www.ingentaconnect.com/content/aalas/cm/2004/00000054/00000006/art00006?crawler=true
15. *215-widefield-fluorescence @ ibidi.com*. (n.d.). Retrieved from https://ibidi.com/content/215-widefield-fluorescence
16. Russell, J. T. (2011). Imaging calcium signals in vivo: A powerful tool in physiology and pharmacology. *British Journal of Pharmacology*, *163*(8), 1605–1625. https://doi.org/10.1111/j.1476-5381.2010.00988.x
17. Gee, K. R., Brown, K. A., Chen, W. N. U., Bishop-Stewart, J., Gray, D., & Johnson, I. (2000). Chemical and physiological characterization of fluo-4 Ca^{2+} -indicator dyes. *Cell Calcium*, *27*(2), 97–106. https://doi.org/10.1054/ceca.1999.0095
18. *axio-zoom-v16-for-materials @www.zeiss.com*. (n.d.). Retrieved from https://www.zeiss.com/microscopy/us/products/stereo-zoom-microscopes/axio-zoom-v16-for-materials.html
19. Berkowski, K. L., Plunkett, K. N., Yu, Q. & Moore, J. S. Introduction to Photolithography: Preparation of Microscale Polymer Silhouettes. *J. Chem. Educ.* **82**, 1365 (2009).
20. Lee, J. B., Choi, K. H. & Yoo, K. Innovative SU-8 lithography techniques and their applications. *Micromachines* **6**, 1–18 (2015).

21. SU-8 photolithography Baking - Elveflow. Retrieved from: https://www.elveflow.com/microfluidic-tutorials/soft-lithography-reviews-and-tutorials/how-to-get-the-best-process/su-8-photolithography-baking/
22. Epoxy, P. & Photoresist, N. Permanent Epoxy Negative Photoresist. (2000) Retrieved from www.microchem.com
23. Palchesko, R. N., Zhang, L., Sun, Y. & Feinberg, A. W. Development of Polydimethylsiloxane Substrates with Tunable Elastic Modulus to Study Cell Mechanobiology in Muscle and Nerve. **7**, (2012).
24. Gale et al. A Review of Current Methods in Microfluidic Device Fabrication and Future Commercialization Prospects. (2018). doi:10.3390/inventions3030060
25. Kamei, K. ichiro, Mashimo, Y., Koyama, Y., Fockenberg, C., Nakashima, M., Nakajima, M., … Chen, Y. (2015). 3D printing of soft lithography mold for rapid production of polydimethylsiloxane-based microfluidic devices for cell stimulation with concentration gradients. *Biomedical Microdevices*, *17*(2). https://doi.org/10.1007/s10544-015-9928-y
26. The Luciferase Reporter Assay – How It Works (n.d.). Retrieved from https://bitesizebio.com/10774/the-luciferase-reporter-assay-how-it-works/
27. Burns, S. M., Vetere, A., Walpita, D., Dančík, V., Khodier, C., Perez, J., … Altshuler, D. (2015). High-throughput luminescent reporter of insulin secretion for discovering regulators of pancreatic β-cell function. *Cell Metabolism*, *21*(1), 126–137. https://doi.org/10.1016/j.cmet.2014.12.010